

We are IntechOpen, the world's leading publisher of Open Access books Built by scientists, for scientists

6,900

Open access books available

185,000

International authors and editors

200M

Downloads

Our authors are among the

154

Countries delivered to

TOP 1%

most cited scientists

12.2%

Contributors from top 500 universities



WEB OF SCIENCE™

Selection of our books indexed in the Book Citation Index
in Web of Science™ Core Collection (BKCI)

Interested in publishing with us?
Contact book.department@intechopen.com

Numbers displayed above are based on latest data collected.
For more information visit www.intechopen.com



Composite Materials with Natural Fibers

*Nicholas Lambrache, Ora Renagi, Lidia Olaru
and Brian N'Drelan*

Abstract

The materials involved in the fabrication of biocomposites have dissimilar physical and chemical properties. More important, the newly created materials exhibit anisotropy and their performance is strongly influenced by the hydrophobic nature of the natural fibers used as reinforcement materials. Beyond a compressive discussion regarding the potential of composite materials with natural fibers in engineering applications, the chapter focuses on simulation of their behavior under applied loads. Modern experimental approaches for defining and validating computer simulations are also introduced. Finally, health hazards and biodegradability issues are evaluated. The new trends in biocomposites materials for engineering applications are briefly discussed.

Keywords: biocomposites classification, anisotropy, hydrophoby, simulation and experimental trends, health hazards

1. Introduction

Environmental and economic considerations recommend the employment of natural fibers as reinforcements in polymeric matrices. The matrix protects the fibers from environmental degradation and by doing so it preserves its mechanical strength. Natural fibers have lower density than artificial fibers, are a renewable material and in most cases are recyclable. The absolute tensile strength of natural fibers is lower than the tensile strength of artificial fibers, as shown in the schematic representation from **Figure 1**. However, due to their lower density, natural fibers have a higher specific tensile strength – defined as the ratio between the absolute tensile strength and the mass density – which makes them ideal candidates for composites employed in aerospace applications.

There are important variations in the physical and chemical properties of natural fibers, variations depending on age, geographical location and age. Such variations must be considered in any design and evaluation of composites with natural fibers and statistical evaluations of strength are important.

Natural fibers are hydrophobic and anisotropic. Such properties pose challenges to the designer and manufacturer of biocomposites. The need to control the content of water in natural fibers requires specific chemical treatment in order to maximize the bond fiber-matrix. The mechanical properties of biocomposites need to be rigorously evaluated by precision experiments and statistical evaluations designed

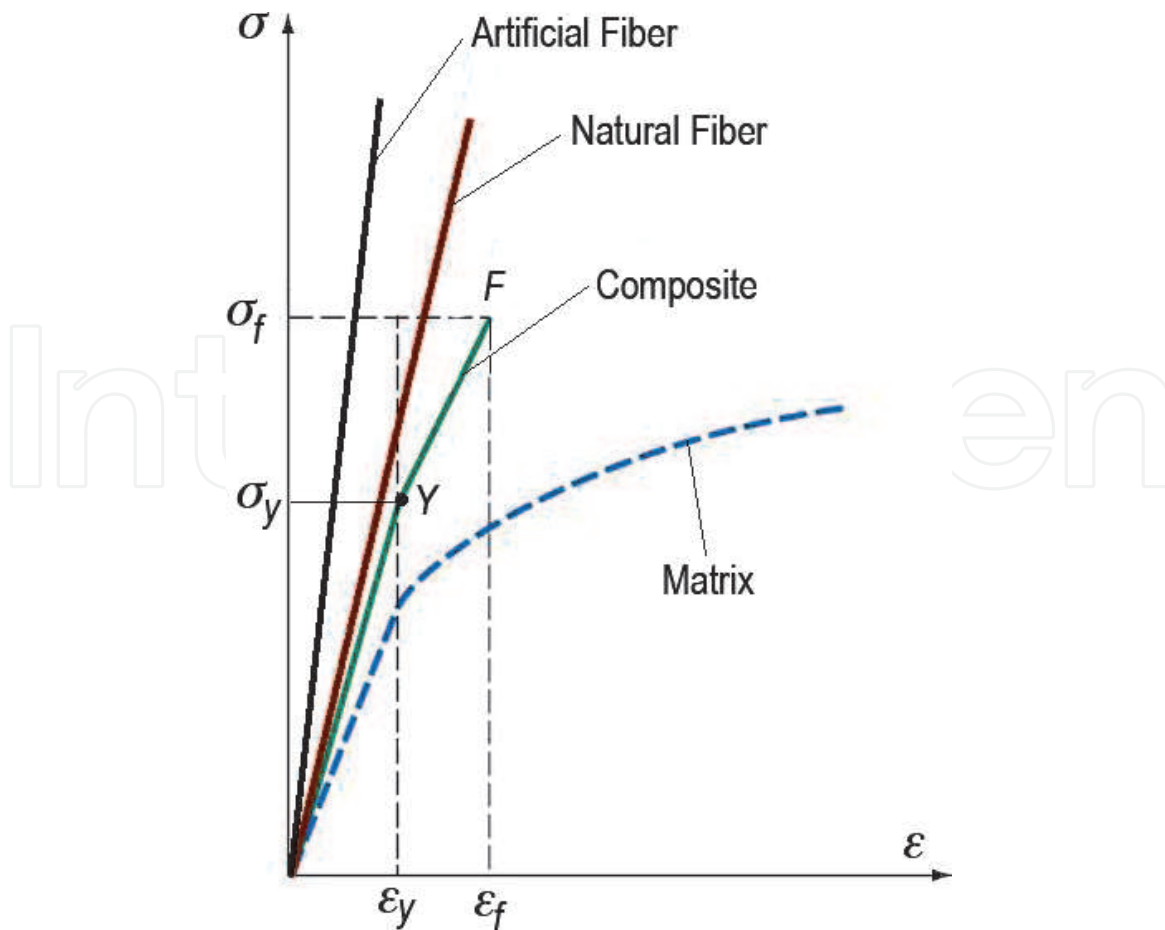


Figure 1.
Stress-strain plots for composites.

to assure reliable input parameters for the computer modeling and simulation of components made from such materials.

This chapter introduces the reader to key aspects encountered in the classification of natural fibers. The performance evaluation, benefits and disadvantages of designing, manufacturing and employment of biocomposites in a wide range of industrial applications are also discussed in some detail.

2. Classification of natural fibers

Natural fibers are the result of geological processes or are produced in the bodies of plants and animals. A general but not exhaustive evaluation of such fibers as potential reinforcing materials in composites is based on their origin:

- Fibers resulted from geological processes. A notable example is asbestos.
- Fibers of animal origin. Such fibers include silk, wool, mohair and alpaca fiber.
- Plant fibers. Such fibers include seed fibers, leaf fibers, bast fibers, fruit fibers and stalk fibers.

2.1 Fibers resulted from geological processes

Asbestos is the only natural fiber produced by geological processes widely used as reinforcement in composite materials. It is a fibrous silicate mineral. There are six types of such fibrous minerals, including amosite, crocidolite, tremolite, chrysotile,

vermiculite and actinolite. All types of fibrous silicate minerals belonging to asbestos family are composed of long, thin crystals, each one composed of a multitude of microscopic fibrils that are easily released into atmosphere. Their inhalation triggers lung health conditions including mesothelioma, asbestosis and cancer, see [1]. For such reasons composites with asbestos are completely banned in many countries. One characteristic sample of chrysotile asbestos from the biggest asbestos mine in the world – Jeffrey Mine, Quebec, Canada, is shown in **Figure 2**. Chrysotile asbestos belongs to the family of serpentine minerals.

2.2 Animal fibers

The most commonly used animal fibers are the wool of domestic sheep and the silk. Other common animal fibers are alpaca fibers and mohair from Angora goats. The silk fiber is secreted by glands located near the mouth of some specific insects during the preparation of their cocoons.

All animal fibers contain specific proteins such as collagen, keratin and fibroin. Collagen is the main structural protein in connective tissues and the most abundant protein in mammals, see [2]. Keratin belongs to the family of structural proteins and is a key structural component of hair, horns, claws or skin in vertebrates, see [3]. In silk, keratin confers excellent tensile strength to the fiber, in the range 650 MPa–750 MPa, see [4]. Regardless of their great importance in bioscience, both wool and silk are less used in the fabrication of composite materials for industrial applications compared with plant fibers.

2.3 Plant fibers

Plant fibers can be collected from leaves, bast, fruit, seeds or stalks. Common leaf fibers include abaca and sisal. Leaf fibers are characterized by increased strength, most likely due to their high content of lignin, see [4]. The most remarkable type of fruit fiber is the coir of coconuts. Bast fibers are part of the outer cell layers of stems of plants and known examples include Kenaf and hemp. Specific plant fibers used as reinforcement in composite materials:

- Bast Fibers: Flax, Kenaf, Jute, Hemp, Pandanus
- Leaf Fibers: Abaca, Pineapple, Banana, Sisal



Figure 2.
Chrysotile from Jeffrey mine, Quebec, Canada. Author's collection.

- Fruit Fibers: Coir
- Stalk Fibers: Straws of Wheat, Rice, Bamboo

Plant fibers offer significant advantages over synthetic fibers as reinforcing components. They are renewable, biodegradable, have low densities and lower processing costs. However, they also bring design and fabrication challenges, mostly due to their reduced adhesion to the polymer matrices as a consequence of their hydrophilic character, see [5]. Some images of plants and the related fibers are shown below. The roots of Pandanus – *Pandanus Utilis* – form a pyramidal tract and it holds the trunk of the plant. Pandanus trees grow in tropical and sub-tropical coastlines and islands of all oceans and can withstand salt spray, drought and strong winds, see [6, 7]. The plants growing along seashores have thick aerial roots as anchors in the sand. Such roots keep the trees upright and secure them in the ground - see **Figure 3**.

The Coconut Palmtree is known for its abundance in the equatorial and tropical regions of the world and also for its versatility – see **Figure 4**. The *Cocos Nucifera* or Coconut Palmtree belongs to the family *Arecaceae*, genus *Cocos* [8]. The drupes are used for food, charcoal, oil and cosmetics, and also in the fabrication of biofuel and composite materials. The mechanical strength of the husk fibers is investigated in many research centers around the world [9–12] and the results show widely distributed values.

The coir or coconut fiber is extracted from the outer husk of the fruit. It has a low density, is unsinkable and resistant to saltwater. The individual fiber cells are narrow and hollow, with thick walls made of cellulose – see **Figure 5**. They are pale when immature, but later become hardened and yellowed as a layer of lignin is



Figure 3.
Pandanus tree from rainforest habitat, PNG University of Technology campus, Lae, Morobe, Papua New Guinea. Inlet: Pandanus Fibers.



Figure 4.
Coconut Palmtree from PNG University of Technology campus, Lae, Morobe, Papua New Guinea. Inlet: Coir.

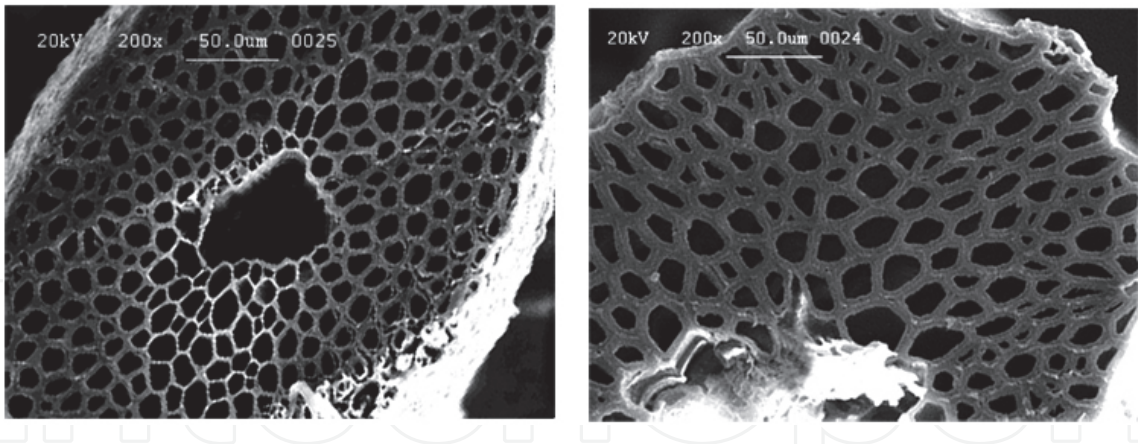


Figure 5.
Cross sections of coir - left - and sisal Fibers – Right – at 200X magnification. Scan electron microscopy on SEMoscope Inovenso IEM 11.

deposited on their walls. Each cell is about 1 mm (0.04 in) long and 10 to 20 μm in diameter. Fibers are typically 100 to 200 mm long. The two varieties of coir are brown and white. Brown coir harvested from fully ripened coconuts is thick, strong and has high abrasion resistance.

Sisal - botanical name *Agave Sisalana* - is a flowering plant native to Yucatan but widely naturalized in many tropical and subtropical regions of the world. The fibers are extracted from the sword-shaped leaves – see **Figure 6**. During its life of 8 to 10 years, the plant grows hundreds of leaves, each one containing around one thousand fibers [13]. Sisal has been the leading material for binder twine for centuries due to its strength, durability, ability to stretch, and resistance to deterioration



Figure 6.
Agave Sisalana from PNG University of Technology campus, Lae, Morobe, Papua New Guinea. Inlet: Sisal Fibers.

in saltwater. However, its traditional use is limited by the competition from polypropylene and the increased potential as reinforcement in composite materials.

The most important constituents of plant fibers are cellulose, hemicellulose, pectin and lignin. Cellulose is an organic polymer with chemical formula $(C_6H_{10}O_5)_n$. The high tensile strength of plant stems arises from the arrangement of cellulose fibers and their distribution into the lignin matrix. Cellulose is responsible for the hydrophilic nature of plant fibers. Hemicellulose is a heteropolymer present along cellulose in all terrestrial plant cell walls, see [14]. Hemicellulose has a random, amorphous structure with little strength, is not resistant to hydrolysis and can be easily hydrolyzed by dilute acid or base. Pectin has the function of holding plant fibers together. Lignin is an organic polymer made by cross-linking phenolic precursors, see [15]. It allows the development of structural materials in the cell walls, lending them strength. In addition, lignin is resistant to decay and its contribution to water absorption is negligible. At low magnifications on scan electron microscopes cross sections of coir and sisal fibers reveal similar honeycomb structures constituted of cellulose fibers in lignin matrices, see **Figure 5**.

3. Technology trends on composite materials with natural fibers

The resins used in manufacturing composite materials can be thermosetting and thermoplastic. The thermosetting resins are predominant, while the thermoplastic resins play a minor role in the fabrication of advanced composites.

The thermosetting resins require the addition of a curing hardener. Once cured, the composite cannot be reformed. Widely used thermosetting resins include epoxies, polyurethanes, phenolic and amino resins and polyamides. The most

common employed are the epoxies because the potential for respiratory exposure is low due to their relatively high molecular-weight.

Another essential component of the cured resins is the hardener. Such compounds control the reaction rate and greatly influence the properties of the matrix. Some commonly used curing agents are the aromatic amines. Like epoxies, such hardeners have a low vapor pressure and are not a respiratory hazard. However, both epoxies and hardeners are a dermal hazard and can even permeate common protective gloves.

The authors of this chapter performed extensive experiments with epoxy resins and hardeners from Struers GmbH, Hanover, Germany. Their epoxy resins are suitable for the matrix of composite materials because they have low shrinkage and the adhesion to natural fibers is excellent. The hardened epoxy is duro-plastic and not affected by moderate heat or chemicals. The curing time is relatively long, but adhesion to most materials is excellent. They polymerize through a chemical reaction after being mixed in the correct proportions. Our experiments employed the polymer Epichlorhydrin in a ratio 15/2 with the hardener Triethylenetetramine. The hardened epoxy is duro-plastic and not affected by moderate heat or chemicals [16].

The curing of epoxy matrix depends on the amount of resin. If small amounts of resin are employed, the polymerization takes longer. However, favorable conditions exist for removing excessive heat generated by the chemical reaction. Larger amounts of epoxy will accelerate the curing process by storing heat due to the poor conductive properties of the system. The air bubbles developed during the curing are caused by higher than acceptable temperatures. Sticky or rubbery sample surfaces after curing indicate a process temperature too low and can be corrected by post-curing in ovens at temperatures below 50°C. The content of water in natural fibers can significantly influence the bond fiber-matrix and it can be reduced by combined exposure to heat at around 120°C for 2 hours and immersion in 10% NaOH for 4 hours. The immersion of fibers in NaOH is increasing the exposed surface, with beneficial effects for their adhesion to the matrix material.

4. Stress behavior simulation of composite materials with natural fibers

All major software platforms for Computer Aided Design and Finite Element Method Simulations allow the study of composites with natural fibers via the Composite Shell implementation. There are three types of composite options to define the arrangement of plies, thicknesses, material properties, and orientations, see **Figure 7**.

- An asymmetric laminate has an asymmetric arrangement of plies about the mid-surface. This is the most general composite option. A schematic of an asymmetric laminate with five layers is shown. Different colors represent different material properties and orientations. The shell mesh is created at the mid-plane.
- A symmetric laminate has a symmetric arrangement of plies - materials, ply orientations, and thicknesses - about the mid-surface. This implies symmetric ply thicknesses, material properties, and material orientations about the mid-plane.
- The sandwich composite is a particular case symmetric laminates with three layers. Such laminates are employed when higher resistance to bending loads is required. The outer two plies are recommended to be stiffer, stronger, and thinner than the middle ply. The core is usually lighter to reduce the overall

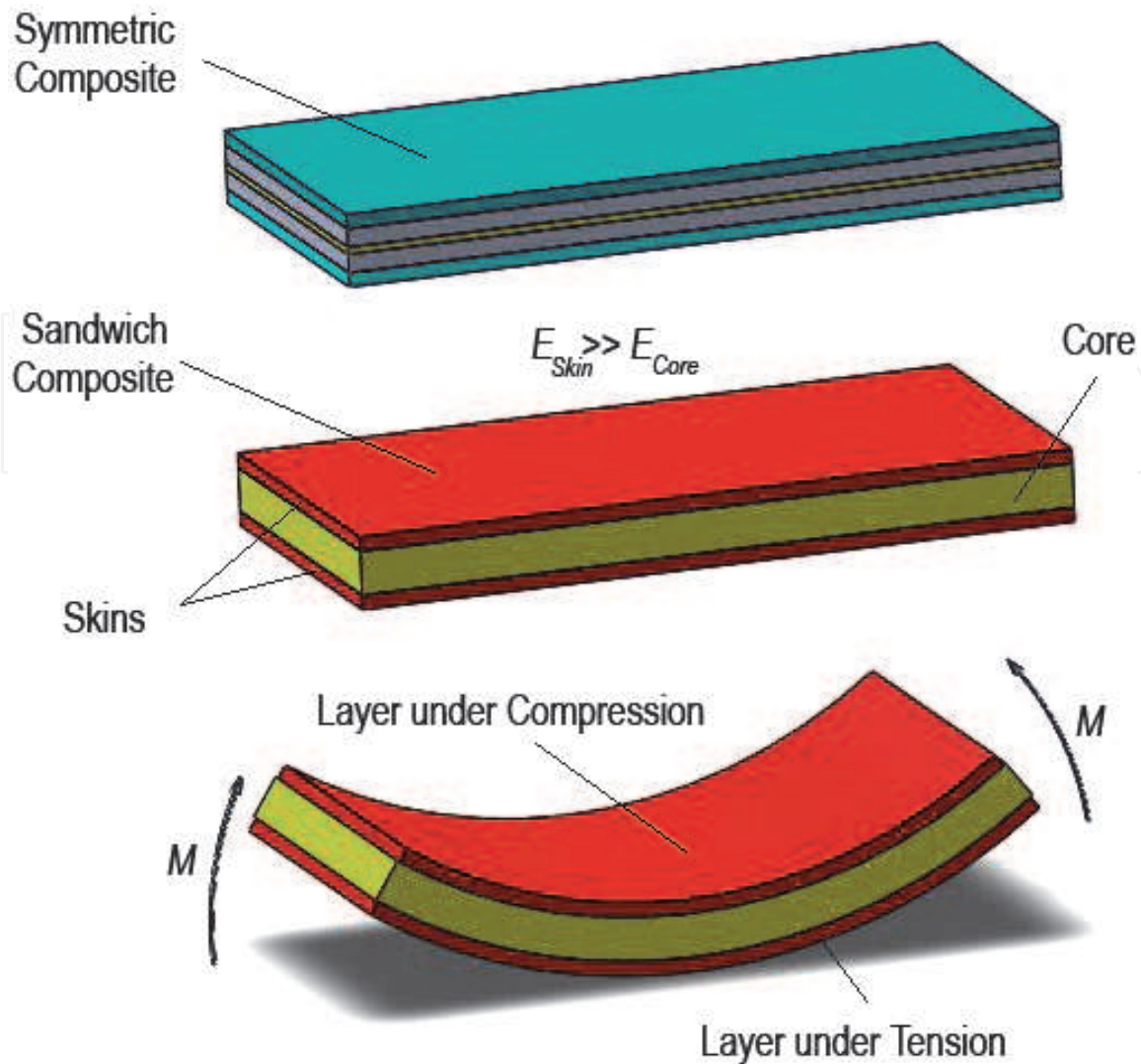


Figure 7.
3D CAD models of symmetric and Sandwich composites.

mass of the composite and has a high shear modulus of elasticity to resist the sliding of the skins.

Composite shells are used for structural members with weight savings required. The shells offer improved fatigue strength, corrosion resistance, and thermal conductivity. In the Shell Property Manager of such applications it is possible to define symmetric, asymmetric or sandwich composites with a number of layers up to 50. The Property Manager also allows users to set different thicknesses, material orientations and same or different material properties for each ply.

Composite laminates are special orthotropic materials that are modeled as single surfaces with several layers of orthotropic materials. A cross-ply sisal fiber-reinforced polymer is an example of a composite laminate with orthotropic material properties for each ply. A rock is an example of an orthotropic material that does not qualify as a composite. Notable differences between a composite laminate and an orthotropic material body:

Composite Laminate:

- Uses a laminated shell element formulation. In addition to other stress results, displays interlaminar shear stress between two adjacent plies. Delamination can occur between two plies with high stress values.

- Uses these unique failure criteria: Tsai-Hill, Tsai-Wu and Maximum Stress

Orthotropic Material Body:

- Uses an element formulation appropriate to the selected body. Interlaminar shear stress components do not apply for bodies defined as orthotropic materials.
- Uses the following failure criteria: Maximum von Mises Stress, Maximum Shear Stress / Tresca, Mohr-Coulomb Stress and Maximum Normal Stress

4.1 Fundamental stress analysis concepts

All system designers must, at early stages, identify the probable failure modes, select a suitable parameter by which severity of loading and environment may be analytically represented, propose a material and geometry for components and implement critical strength properties related to the probable failure mode. The magnitude of the loading severity parameter must be calculated under applicable loading and environmental conditions, and compared with the critical strength property. Failure may be averted by assuring that the loading severity parameter is safely less than the corresponding critical strength property for each potential failure mode.

The most important loading severity parameters are stress, strain, and strain energy per unit volume. Of these, stress is usually selected for calculation purposes. To completely define the state of stress at any selected point within a solid body, it is necessary to describe the magnitudes and directions of stress vectors on all possible planes that could be passed through such point. One way of defining the state of stress at a point is to determine all stress components that can occur on the faces of an infinitesimal cube of material placed at the origin of an arbitrarily selected right-handed Cartesian coordinate system of known orientation. Each of these components of stress may be classified as either a normal stress σ normal to a face of the cube, or a shear stress τ parallel to a face of the cube. The illustration in **Figure 8** depicts all possible stress components acting on an infinitesimal cubic volume element of dimensions $dx-dy-dz$.

Depending upon whether its material behaves in a *brittle* or a *ductile* manner, failure at the governing critical point of a component is dependent upon the principal normal stresses, the principal shearing stresses, or some combination of these. In any event, the designer must evaluate principal normal stresses and principal shearing stresses for any combination of applied loads. To do this, the general stress cubic Eq. (1) may be employed to find the principal stresses $\sigma_1, \sigma_2, \sigma_3$ and as a function of the readily calculable components of stress $\sigma_x, \sigma_y, \sigma_z, \tau_{xy}, \tau_{yz}, \tau_{zx}$ relative to any selected $x-y-z$ coordinate system. The general stress cubic equation, developed from equilibrium concepts, has the form – see [17]:

$$\begin{aligned} \sigma^3 - \sigma^2(\sigma_x + \sigma_y + \sigma_z) + \sigma(\sigma_x\sigma_y + \sigma_y\sigma_z + \sigma_z\sigma_x - \tau_{xy}^2 - \tau_{yz}^2 - \tau_{zx}^2) - \\ - (\sigma_x\sigma_y\sigma_z + 2\tau_{xy}\tau_{yz}\tau_{zx} - \sigma_x\tau_{yz}^2 - \sigma_y\tau_{zx}^2 - \sigma_z\tau_{xy}^2) = 0 \end{aligned} \quad (1)$$

Since all normal and shearing stress components are real numbers, all three roots of the general stress cubic equation are real. These three roots are the principal normal stresses $\sigma_1, \sigma_2, \sigma_3$. It is also possible to find the directions of principal stress vectors and principal shearing stress vectors if necessary. Furthermore, it can be shown that the magnitudes of the principal shearing stresses may be calculated from Eq. (2):

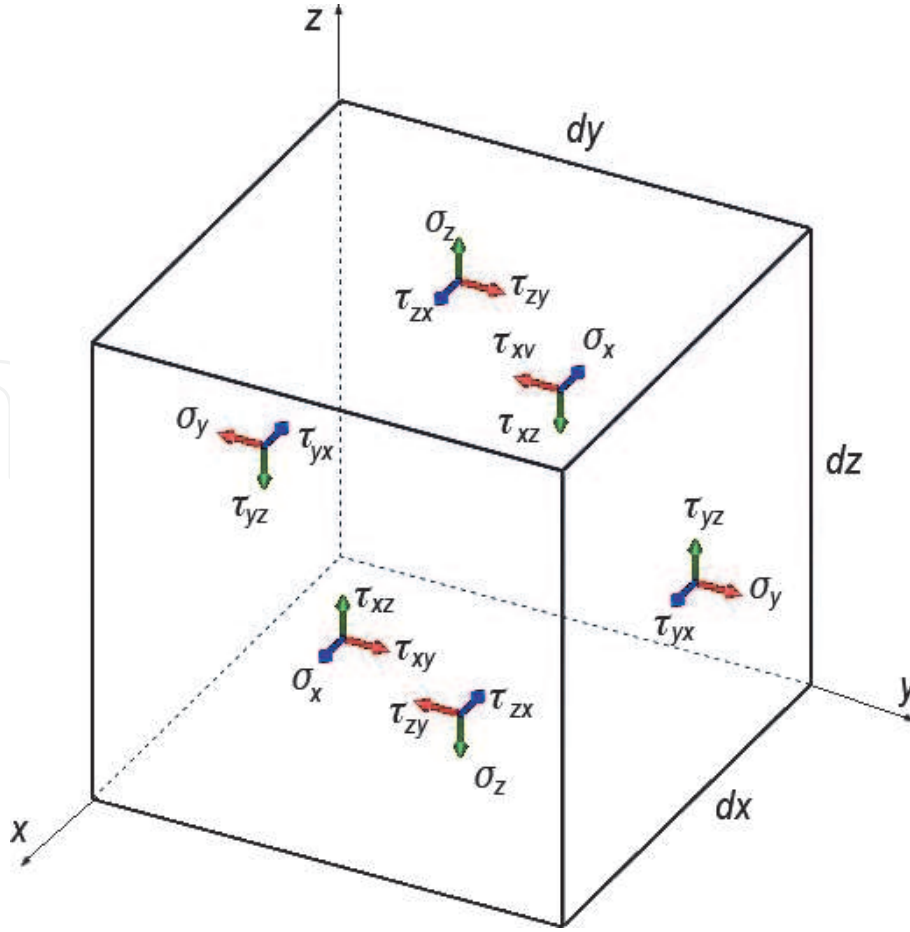


Figure 8.
Complete definition of the state of stress at arbitrary points.

$$|\tau_1| = \left| \frac{\sigma_2 - \sigma_3}{2} \right|, \quad |\tau_2| = \left| \frac{\sigma_3 - \sigma_1}{2} \right|, \quad |\tau_3| = \left| \frac{\sigma_1 - \sigma_2}{2} \right| \quad (2)$$

To summarize, if loads and geometry are known for a component in any system, the designer may identify the critical point, arbitrarily select a convenient x - y - z coordinate system, and calculate the resultant six stress components $\sigma_x, \sigma_y, \sigma_z, \tau_{xy}, \tau_{yz}, \tau_{zx}$. The above equations can be solved to find the principal normal stresses and the principal shearing stresses.

4.2 Failure criteria for composite materials

To determine whether a laminate will fail due to any applied load, the stresses across the different plies needs to be calculated and next a failure criterion based on these stress levels must be selected. The failure of composites occurs in multiple steps. When the stress in the first ply or first group of plies is high enough, it fails. This point of failure is the first ply failure, beyond which a laminate can still carry the load. For a safe design, laminates should be exposed to stresses below this point. The point where the total failure occurs is termed the ultimate laminate failure. Failure of composites occurs on a micromechanical scale due to fiber damage, matrix cracking, or interface or inter-phase failure. The local failure modes mentioned above cannot predict global laminate failure satisfactorily. Composite failure theories predict global laminate failure. These failure theories can be interactive, non-interactive or partially interactive. The non-interactive theories do not consider the interaction between different stress components, whereas the interactive theories do. The three theories available for laminate failure criteria are:

- Maximum Stress Criterion
- Tsai-Hill Failure Criterion
- Tsai-Wu Failure Criterion

The *Maximum Stress Criterion* widely applies to composite shells. Failure occurs according to the maximum stress criterion when the stress in one of the principal material directions exceeds the strength in that direction. The overall state of stress in the global coordinates is first computed by the program. Then, the program computes stress along the principal material directions for each lamina by applying a coordinate transformation. The program assumes a state of plane stress - 2D - for a lamina with $\sigma_3 = 0$, $\tau_{13} = 0$, $\tau_{23} = 0$. The failure index FI is computed as follows:

$$FI = \max \left(\frac{\sigma_1}{S_1}, \frac{\sigma_2}{S_2}, \left| \frac{\sigma_{12}}{S_{12}} \right| \right) \quad (3)$$

The software reports a Factor of Safety $FOS = \frac{1}{FI} = \frac{1}{\max \left(\frac{\sigma_1}{S_1}, \frac{\sigma_2}{S_2}, \left| \frac{\sigma_{12}}{S_{12}} \right| \right)}$. The composite will not fail if $FOS > 1$. The significance of the parameters involved in the equations above is:

- S_1 - Tensile strength of laminate in direction 1
- S_2 - Tensile strength of laminate in direction 2
- S_{12} - Shear strength of laminate

There are some additional requirements:

- If $\sigma_1 > 0$, $S_1 = S_{1 \text{ Tensile}}$
- If $\sigma_1 < 0$, $S_1 = S_{1 \text{ Compressive}}$
- If $\sigma_2 > 0$, $S_2 = S_{2 \text{ Tensile}}$
- If $\sigma_2 < 0$, $S_2 = S_{2 \text{ Compressive}}$

The maximum stress criterion has the following characteristics:

- It does not consider the interactions between different stress components into account as seen from the above equations.
- Predicts specific failure modes since stress in each material principal direction is compared with strength in that direction.

The *Tsai-Hill Criterion* considers the distortion energy portion of the total strain energy that is stored due to loading. The distortion energy is the portion of strain energy that causes shape change. The other portion is the dilatation energy that causes volume or area change due to loading. For composite shells each lamina is assumed to be in a state of plane stress with $\sigma_3 = 0$, $\tau_{13} = 0$, $\tau_{23} = 0$. The failure index is computed as:

$$FI = \frac{\sigma_1^2}{S_1^2} - \frac{\sigma_1\sigma_2}{S_1^2} + \frac{\sigma_2^2}{S_2^2} + \frac{\tau_{12}^2}{S_{12}^2} \quad (4)$$

The significance of the parameters involved in Eq. (4) above is:

- S_1 - Tensile strength of laminate in direction 1
- S_2 - Tensile strength of laminate in direction 2
- S_{12} - Shear strength of laminate

The program reports a Factor of Safety $FOS = \frac{1}{\sqrt{FI}} = \frac{1}{\sqrt{\frac{\sigma_1^2}{S_1^2} - \frac{\sigma_1\sigma_2}{S_1^2} + \frac{\sigma_2^2}{S_2^2} + \frac{\tau_{12}^2}{S_{12}^2}}}$.

The FOS is the coefficient by which all stress components should be multiplied to reach laminate failure at $FI = 1$. The composite will not fail if $FOS > 1$. There are also some additional requirements for this failure criterion:

- If $\sigma_1 > 0$, $S_1 = S_{1 \text{ Tensile}}$
- If $\sigma_1 < 0$, $S_1 = S_{1 \text{ Compressive}}$
- If $\sigma_2 > 0$, $S_2 = S_{2 \text{ Tensile}}$
- If $\sigma_2 < 0$, $S_2 = S_{2 \text{ Compressive}}$

The Tsai-Hill criterion considers the interaction between different stress components. However, it cannot predict various failure modes including fiber failure, matrix failure, and fiber-matrix interface failure.

The *Tsai-Wu Criterion* is applied to determine the factor of safety for composite orthotropic shells. This criterion considers the total strain energy - both distortion energy and dilatation energy - for predicting failure. It is more general than the Tsai-Hill failure criterion because it distinguishes between compressive and tensile failure strengths. For a 2D state plane stress - $\sigma_3 = 0$, $\tau_{13} = 0$, $\tau_{23} = 0$ - the Tsai-Wu failure criterion is expressed as:

$$F_1\sigma_1 + F_2\sigma_2 + 2F_{12}\sigma_1\sigma_2 + F_{11}\sigma_1^2 + F_{22}\sigma_2^2 + F_6\tau_{12} + F_{66}\tau_{12}^2 = 1 \quad (5)$$

The coefficients F_{ij} of the orthotropic Tsai-Wu failure criterion are related to the material strength parameters of the lamina determined by experiments. They are calculated from with following equations:

$$\begin{aligned} F_1 &= \left(\frac{1}{S_{1 \text{ Tensile}}} - \frac{1}{S_{1 \text{ Compressive}}} \right), F_2 = \left(\frac{1}{S_{1 \text{ Tensile}}^2} - \frac{1}{S_{1 \text{ Compressive}}^2} \right), \\ F_{12} &= -\frac{1}{2} \sqrt{\frac{1}{S_{1 \text{ Tensile}}^2 \cdot S_{1 \text{ Compressive}}^2} \cdot \frac{1}{S_{2 \text{ Tensile}}^2 \cdot S_{2 \text{ Compressive}}^2}}, \\ F_{11} &= \frac{1}{S_{1 \text{ Compressive}}^2 \cdot S_{1 \text{ Tensile}}}, F_{22} = \frac{1}{S_{2 \text{ Compressive}}^2 \cdot S_{2 \text{ Tensile}}}, \\ F_6 &= \left(\frac{1}{S_{12 \text{ T}}^2} - \frac{1}{S_{12 \text{ C}}^2} \right), F_{66} = \frac{1}{S_{12 \text{ C}} \cdot S_{12 \text{ T}}} \end{aligned} \quad (6)$$

The significance of the parameters involved in the equations above is:

- $S_{1 \text{ Tensile}}$ - Tensile strength of laminate along fiber direction
- $S_{1 \text{ Compressive}}$ - Compressive strength of laminate along fiber direction
- $S_{2 \text{ Tensile}}$ - Tensile strength of laminate transverse to fiber direction
- $S_{2 \text{ Compressive}}$ - Compressive strength of laminate transverse to fiber direction
- $S_{12 \text{ T}}$ - Positive shear strength of laminate
- $S_{12 \text{ C}}$ - Negative shear strength of laminate, considered equal to the positive shear strength by the solver in Finite Element Analysis. Directions 1 and 2 refer to the fiber direction, respectively transversal to it.

The factor of safety FOS is the coefficient by which all laminate stress components should be multiplied to reach laminate failure according to the Tsai-Wu criterion stated above. The FOS for laminate failure is calculated as:

$$FOS = \frac{R - C_1}{2C_2}, C_1 = F_1\sigma_1 + F_2\sigma_2 + F_6\tau_{12},$$

$$C_2 = F_{11}\sigma_1^2 + F_{22}\sigma_2^2 + F_{66}\tau_{12}^2 + 2F_{12}\sigma_1\sigma_2, R = \sqrt{|C_1^2 + 4C_2|} \quad (7)$$

If $FOS > 1$, the composite will not fail. The Tsai-Wu failure criterion cannot predict different failure modes including fiber failure, matrix failure, and fiber-matrix interface failure.

4.3 Example

Consider a composite material with natural fibers. The composite has seven plies, a layup $[0/90/0/90/0/90/0]$ and it is subject to three point bending with support span of 20 mm by applying a uniform load $P = 10 \text{ N/mm}$ at the center. The objective of the simulation is to evaluate the longitudinal stress S_X , the displacement U_Y at point B and the transverse shear stress T_{XY} at point C. The geometric and mechanical properties of the composite as evaluated by measurement and experiments are:

- Thickness of Pliers 1, 2, 3, 5, 6, 7: $d = 0.1 \text{ mm}$
- Thickness of Ply 4: $d = 0.4 \text{ mm}$
- The fibers on plies are oriented normal to each other, see **Figure 9**.
- Model: Linear Elastic Orthotropic
- Elastic Modulus: $E_X = 1e + 11 \text{ N/m}^2$, $E_Y = 5e + 9 \text{ N/m}^2$, $E_Z = 5e + 9 \text{ N/m}^2$
- Poisson's Ratio: $\nu_{XY} = 0.4$, $\nu_{YZ} = 0.3$, $\nu_{XZ} = 0.3$
- Shear Modulus: $G_{XY} = 3e + 9 \text{ N/m}^2$

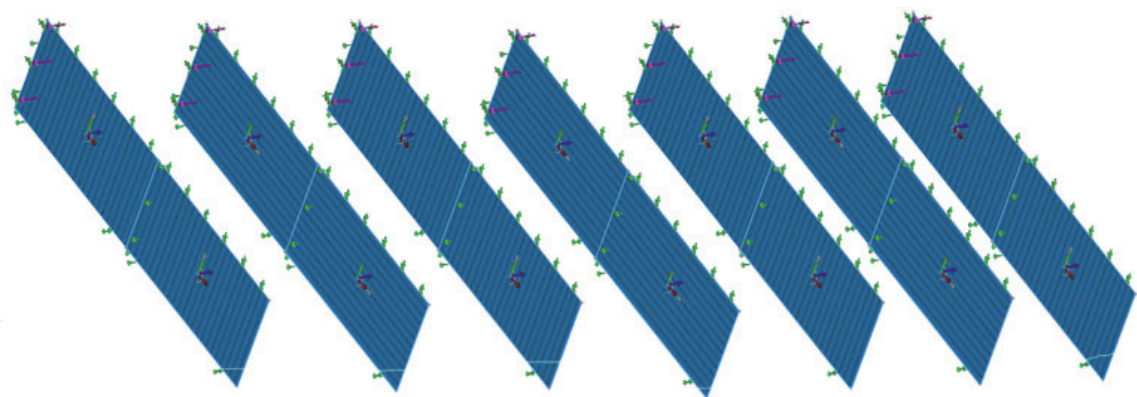


Figure 9.
Plies orientation.

- Mass Density: $\rho = 1400 \text{ kg/m}^3$
- Tensile Strength in X: $S_e = 1.4256e + 8 \text{ N/m}^2$
- Yield Strength: $S_y = 1.3904e + 8 \text{ N/m}^2$
- Default Failure Criterion: Max von Mises Stress [17, 18]
- Due to symmetry, only a quarter of the composite is modeled

The simulation results are shown in **Figure 10** and are validated by experiments.

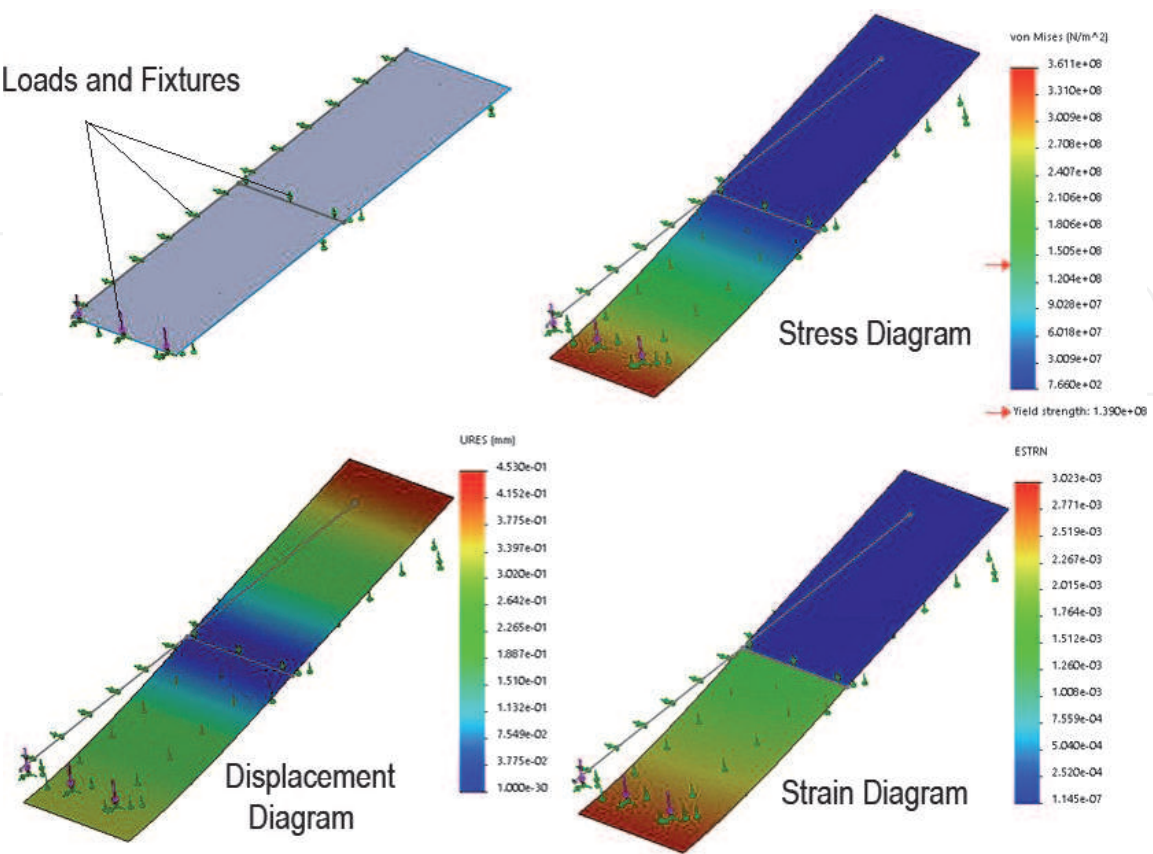


Figure 10.
Stress, displacement and strain diagrams.

5. Modern experimental approaches

Laboratory-scale tensile and torsion testing machines allow experimental evaluations between any applied tensile/torque loads and the induced linear elongations or twist on composite specimens with natural fibers. In engineering terms, they facilitate the experimental evaluation of yield strength, Young modulus E or shear modulus G with accuracy. The specimen can also be brought to the point of destruction and such experiments allow the establishment of the failure point of the material.

Such experiments can be performed with the required precision on SM1002 Bench-Top Tensile Testing Machines and SM1001 Torsion Testing Machines from Tecquipment. The experimental evaluation of Poisson's Ratio with the relationship $\nu = -d\epsilon_t/d\epsilon_a$ performed under EU Standard 10,002-1 directions is also important because it provides input parameters for simulations.

If the fibers are randomly oriented in the matrix may be acceptable to consider the composite a homogenous, isotropic linear elastic material. Under such

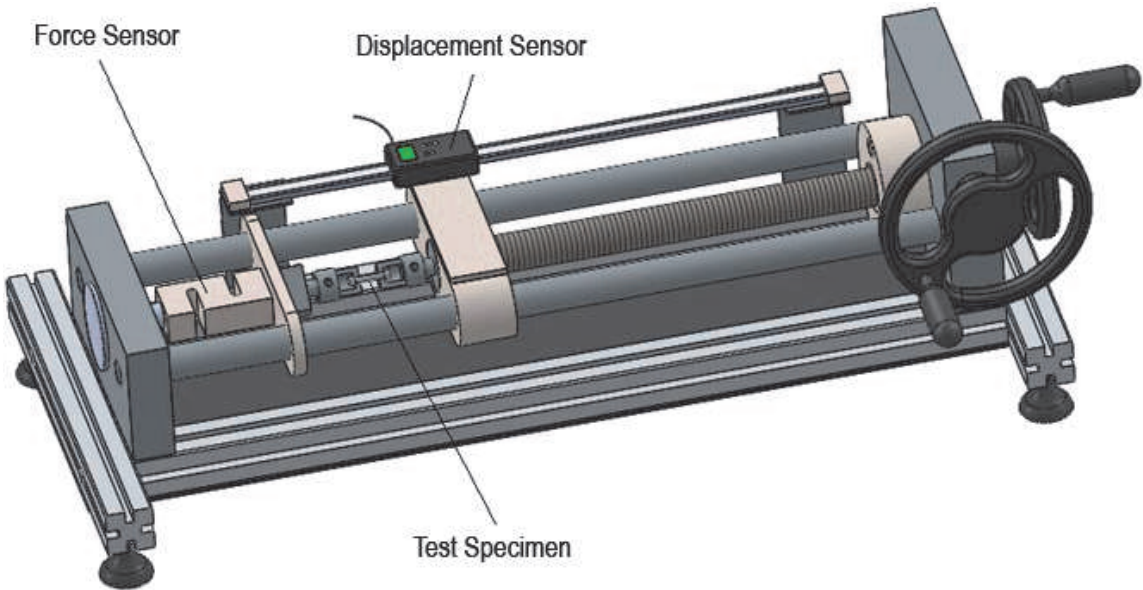


Figure 11.
3D CAD model of tensile testing machine.

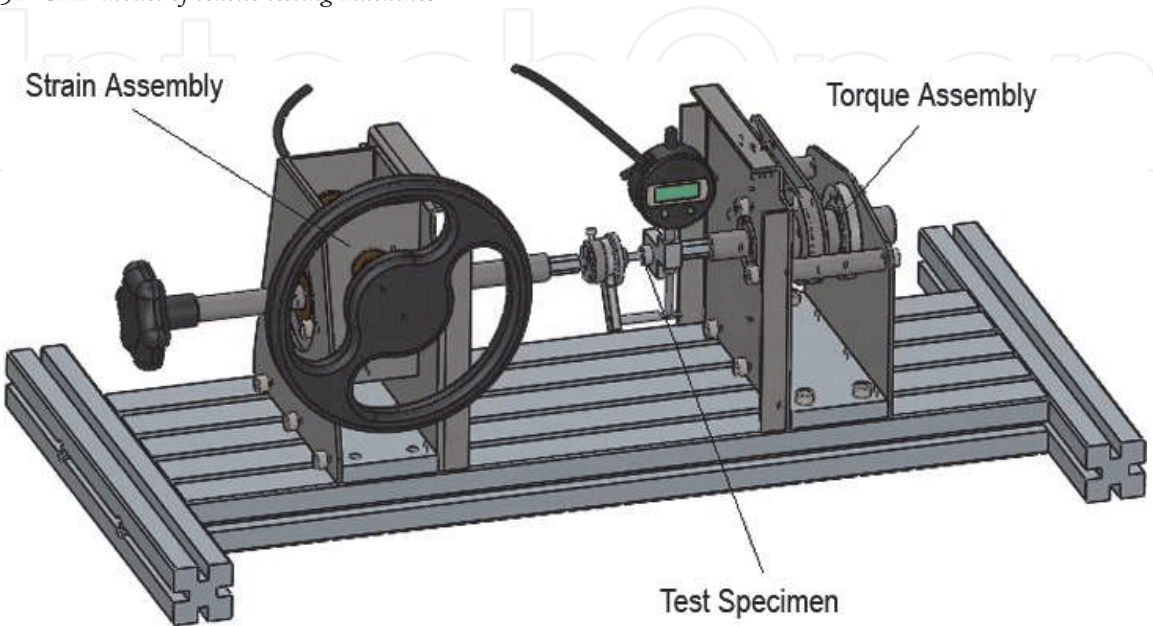


Figure 12.
3D CAD model of a torsion testing machine.

assumptions, the elastic properties of the composite material are fully defined by the Young modulus and shear modulus and the formula involving them allows the calculation of Poisson ratio ν :

$$G = \frac{E}{2(1 + \nu)}, \nu = \frac{E}{2G} - 1 \tag{8}$$

The following pages briefly introduce 3D CAD models of tensile testing, torsion, creep and rotating fatigue computer controlled machine recommended in the experimental research of composite materials with natural fibers – see **Figures 11–14**. Screenshots of specific tests are also introduced in **Figures 15–18**.

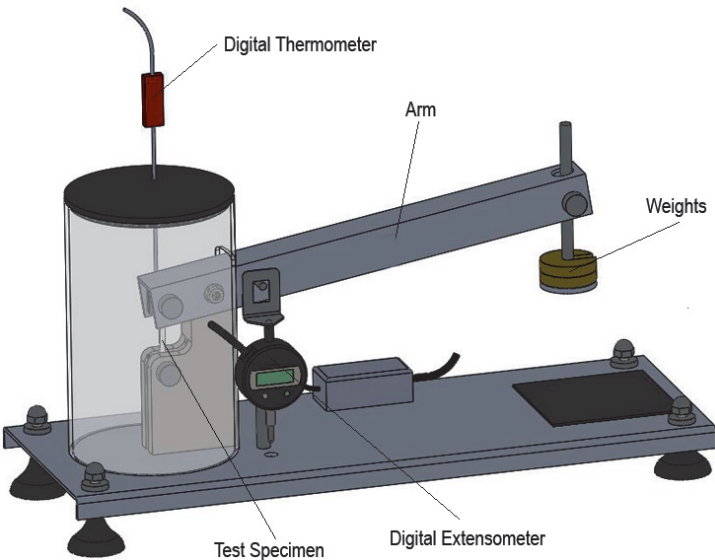


Figure 13.
3D CAD model of a creep testing apparatus.

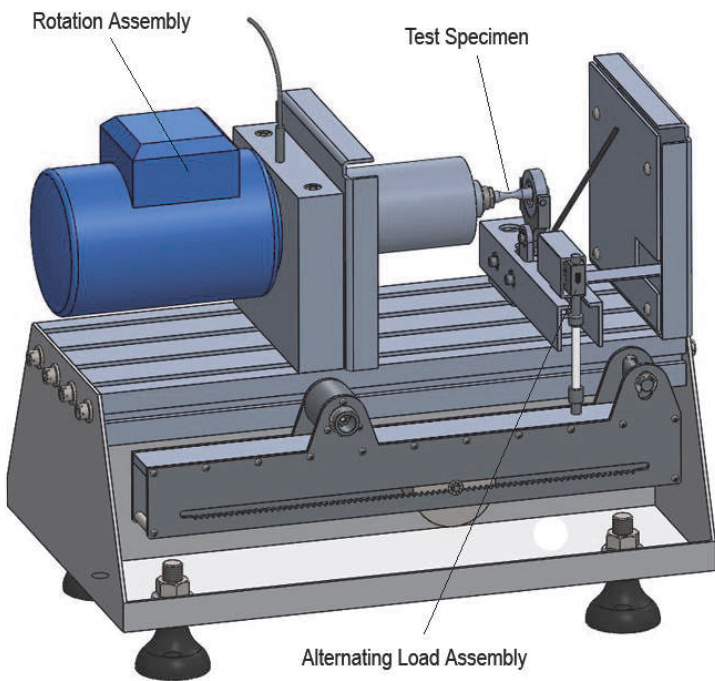


Figure 14.
3D CAD model of a rotating fatigue machine.

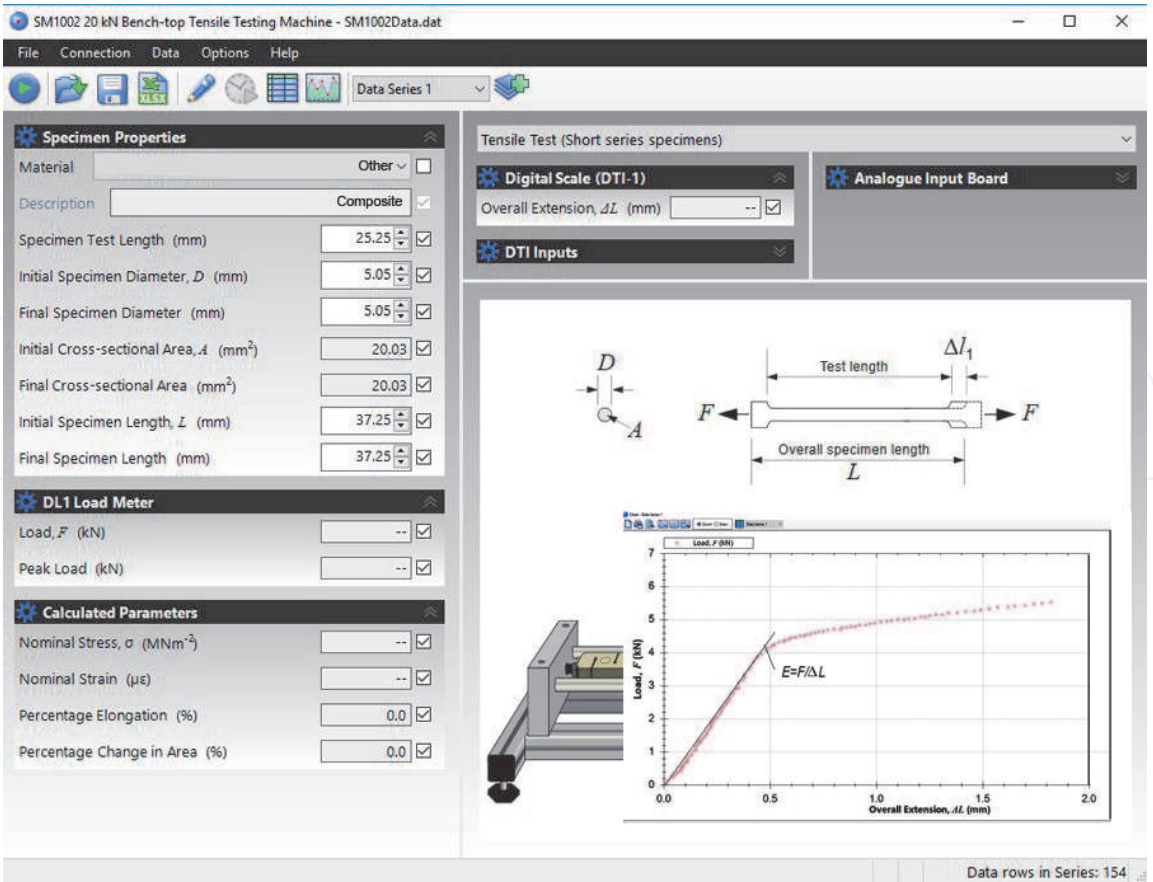


Figure 15.
Tensile test screenshot of a composite material.

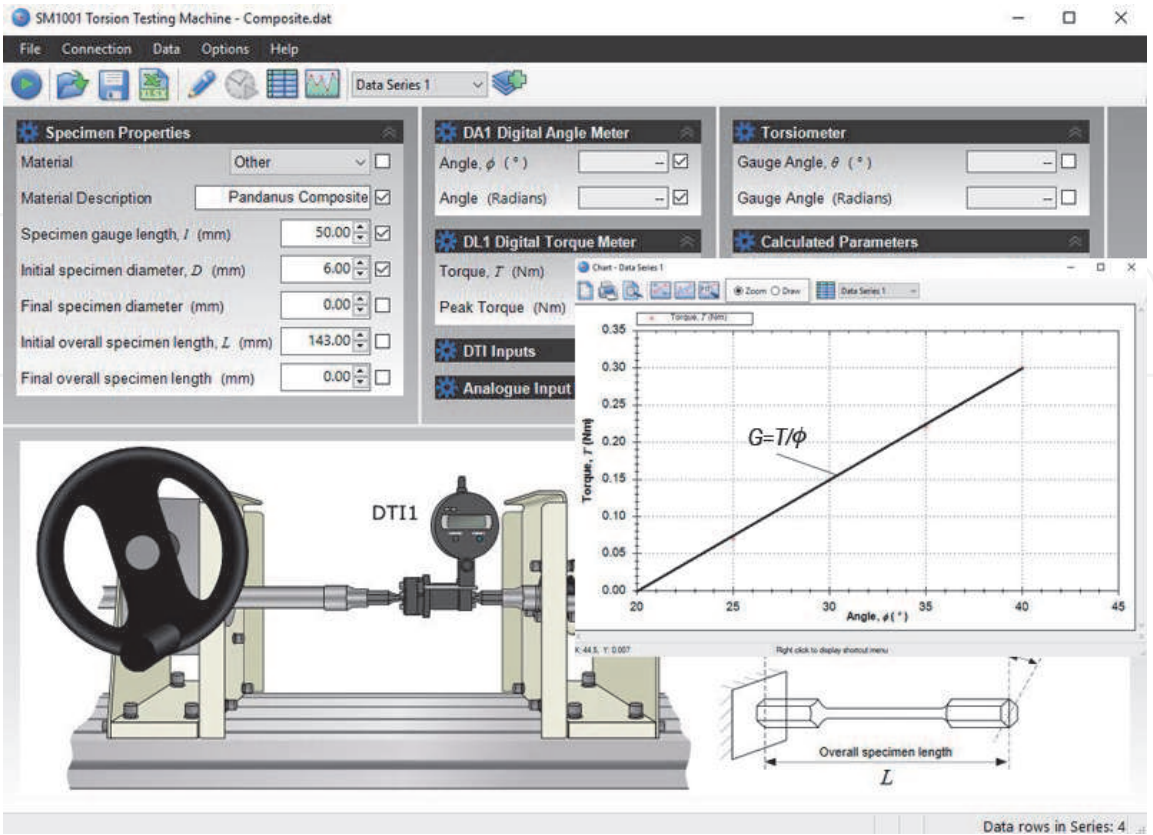


Figure 16.
Torsion test screenshot of a composite material.

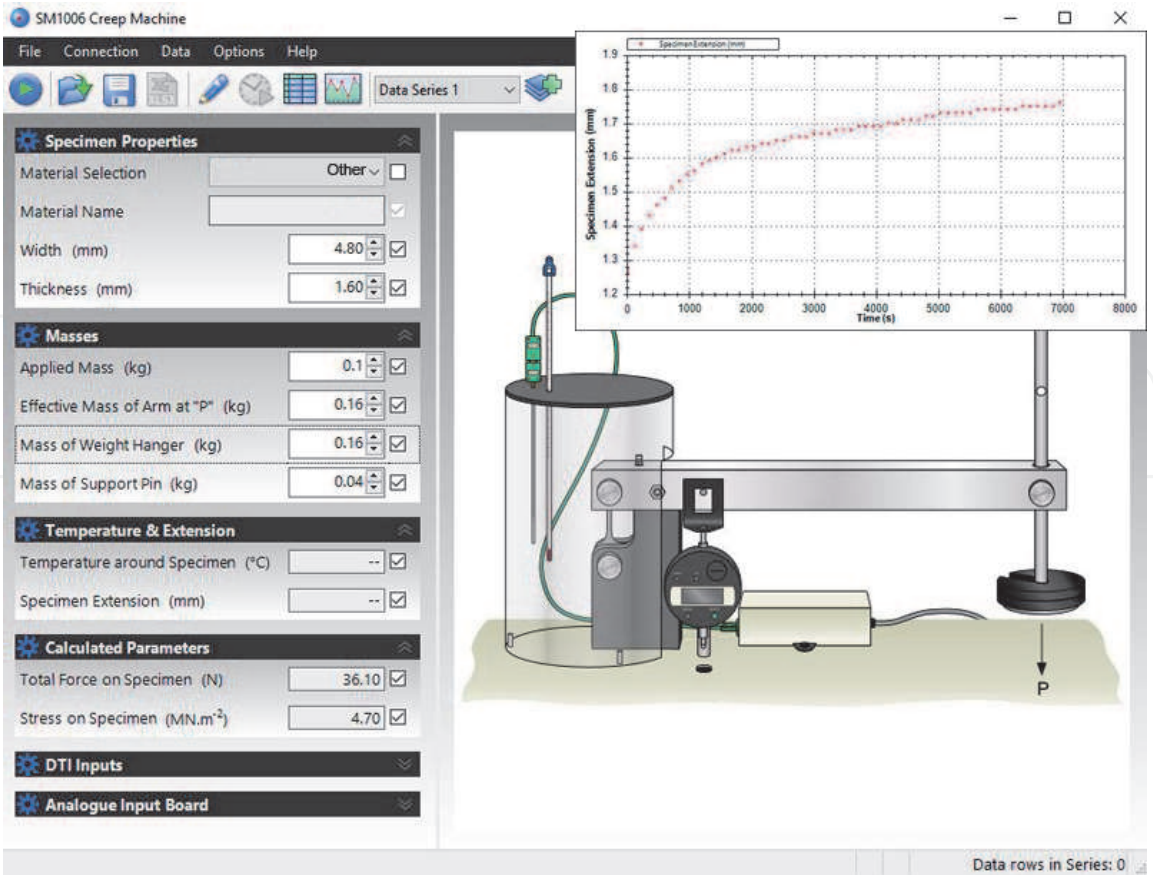


Figure 17.
Creep test screenshot of a composite material.

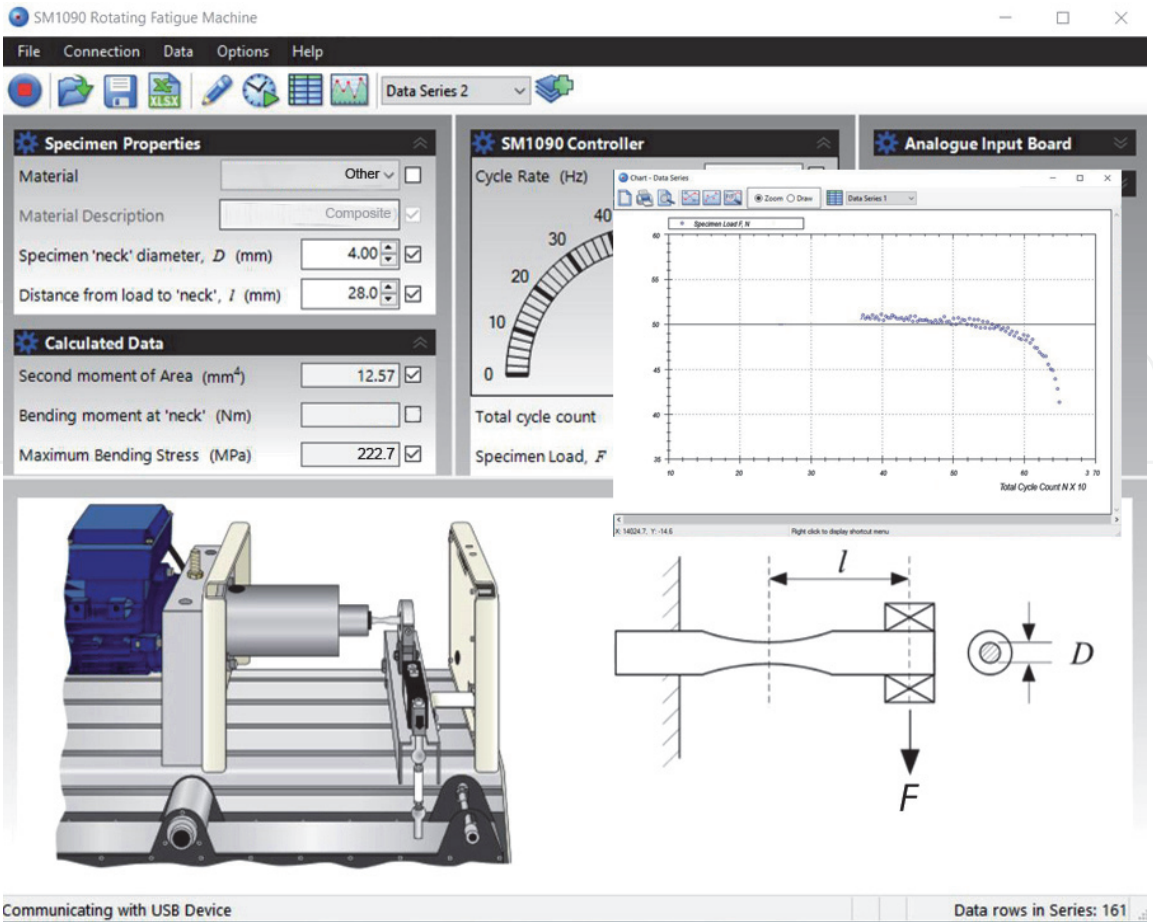


Figure 18.
Fatigue test screenshot of a composite material.

6. Conclusions

Natural fibers show potential as reinforcements in composite materials due to their superior specific strength and their sustainable and recyclable character. Being anisotropic materials, biocomposites are challenging the simulation environments and require advanced and precision experimental equipment. The biohazard aspects of most natural fibers used as reinforcements are minimal. This field of engineering materials is interdisciplinary by its nature and still needs time to mature.

Author details


Nicholas Lambrache^{1*}, Ora Renagi¹, Lidia Olaru² and Brian N'Drelan¹

¹ PNG University of Technology, Lae, Papua New Guinea

² Jesta Group, Montreal, Canada

*Address all correspondence to: Nicholas.Lambrache@pnguot.ac.pg

IntechOpen

© 2022 The Author(s). Licensee IntechOpen. This chapter is distributed under the terms of the Creative Commons Attribution License (<http://creativecommons.org/licenses/by/3.0>), which permits unrestricted use, distribution, and reproduction in any medium, provided the original work is properly cited. 

References

- [1] Luus K. Asbestos: Mining exposure, health effects and policy implications. *McGill Journal of Medicine*. 2006;**10**(2): 121-6
- [2] Fratzl P. Collagen: Structure and Mechanics. New York: Springer. ISBN 978-0-387-73905-2; 2008
- [3] Wang B. Keratin: Structure, mechanical properties, occurrence in biological organisms, and efforts at bioinspiration. *Progress in Materials Science*. 2016;**76**:229-318
- [4] Quazi T, Alam K, Quaiyyum M. Mechanical properties of polypropylene composites: A review. *Journal of Thermoplastic Composite Materials*. 2011;**26**(3):362-391
- [5] Fazeli M, Florez J, Simão R. Improvement in adhesion of cellulose fibers to the thermoplastic starch matrix by plasma treatment modification. *Composites Part B: Engineering*. 2018; **163**:207-216
- [6] Hyndman D. Ethnobotany of Wopkaimin Pandanus significant Papua New Guinea plant resource. *Economic Botany*. 1984;**38**:3
- [7] St. John H. Revision of the Genus Pandanus Stickman: New Papuan species in the section microstigma collected by C. E. Carr. *Pacific Science*. 1968;**22**:4
- [8] Thampan PK. Handbook on Coconut Palm. London: Oxford & IBH Publishing; 1981
- [9] Bledzki AK, Gassan J. Composites reinforced with cellulose based fibers. *Progress in Polymer Science*. 1999; **24**(2):221-274
- [10] Li X, Tabil TG, Panigrahi S. Chemical treatments of natural fiber for use in natural fiber-reinforced composites: A review. *Journal of Polymers and the Environment*. 2007; **15**:25-33
- [11] Guadalupe M. Preparation and characterization of biodegradable composites based on Brazilian cassava starch, corn starch and green coconut fibers. *Carbohydrate Polymers*. Vol. 80. Rio de Janeiro, Brazil: Matera. 2010. DOI: 10.1590/S1517-70762010000200034. Available from: <https://www.scielo.br/j/rmat/a/MZ3bN4x3thCJm3j8mYck7Km/?lang=en>
- [12] Awang L. Mechanical properties and microstructure of coconut coir fibers. In *Proceeding of MAMIP2012 Asian International Conference on Materials, Minerals and Polymer*. 23rd – 24th March 2012, Penang: Research Gate; 2012. Available from: https://www.researchgate.net/publication/236263388_Mechanical_Properties_and_Microstructure_of_Cocos_Nucifera_Coconut_Coir_Fibres
- [13] Gentry HS. Agaves of Continental North America. Arizona, United States: University of Arizona Press; 1982. pp. 628-631
- [14] Scheller H, Ulvskov P. Hemicelluloses. *Annual Review Plant Biology*. 2010;**61**:263-289
- [15] Lebo S, Gargulak J, McNally T. Lignin, Kirk-Othmer Encyclopedia of Chemical Technology. New Jersey, United States: John Wiley & Sons; 2001
- [16] Lambrache N, Pumwa J, Renagi O, Olaru L, N'Drelan B. Stress behavior of composite materials with natural fibers from the South Pacific. In: *Proceedings of the International Conference on Industrial Engineering and Operations Management*. Paris, France, United States: IEOM Society International; 2018. pp. 3197-3207
- [17] Cook RD. Concepts and Applications of Finite Element Analysis. 2nd ed. New Jersey, United States: John Wiley & Sons; 1981

[18] Von Mises R. Mechanik der festen Körper im plastisch deformablen Zustand. In: Göttingen N. Mathematik Physics. Vol. 1913. France: European Digital Mathematics Library; 1913. pp. 582-592. Available from: <https://eudml.org/doc/58894>

IntechOpen

IntechOpen